Analysis of Dense-Mesh Distribution Network Operation Using Long-Term Monitoring Data

Michal Ptacek [1],* [ID], Vaclav Vycital [1] [ID], Petr Toman [1] [ID] and Jan Vaculik [2]

[1] Department of Electrical Power Engineering, Brno University of Technology, Technicka 12, 61600 Brno, Czech Republic; vycital@feec.vutbr.cz (V.V.); toman@feec.vutbr.cz (P.T.)

[2] E.ON Distribuce, a.s., Hady 2, 61400 Brno, Czech Republic; jan.vaculik@eon.cz

* Correspondence: ptacekm@feec.vutbr.cz; Tel.: +420-541-146-209

Abstract: The technical and economic aspects and the possibility of the mesh network topology offering many radial configurations lead to the fact that large municipal networks are generally under radial operation. However, it is very important to analyze the operation and control of the mesh networks, especially in terms of their safety and durability and in the frame of the smart grid concept, respectively. The article deals with the analysis of the operation of the dense-mesh municipal distribution network of E.ON Distribuce a.s. based on the long-term data from power quality monitors. It also shows a brief view of the current lack of data usability from monitors installed in distribution networks in the context of smart grid.

Keywords: dense-mesh topology; municipal distribution network; smart grid; power quality monitor; long-term; operation analysis

1. Introduction

One of the main outcomes resulting from the transition towards new smart grids is expected the better observability and monitoring of the whole grid [1]. This observability is expected due to the bulk installation of smart meters, as well as the monitoring of transformer stations, ring main units, etc. [1,2]. Even though there is still lot of concern and research devoted to the processing of such a huge amount of recorded data [3] and its reliable communication back to distribution system operator database [4,5], the usefulness of measurement data availability is already obvious [1,2,6–11]. One of the fields that will benefit from the detailed measurement data availability would be distribution system modelling, planning, and operation optimization [1,6,7,11–14], which will be more accurate.

A commonly performed task as part of distribution system planning is the calculation of load flow. Although the solution of a non-linear power flow problem is quite well addressed [15–17], there is still some effort mainly devoted in computational and time efficiency of this numerically intensive task [18]. A part of load flow studies is also appropriate the modelling of connected loads, which can be as with constant impedance, constant current, or constant power, i.e., ZIP load model [19]. Basically, the historical data are very useful in the case of modelling verification, as well as the mapping of possible extreme states of the network. Thus, it is expected that the availability of more accurate data from bulk deployment of measurement will definitely lead to more accurate load models, power flow studies, load forecasting, prosumers tariffs setting, etc.

However, data processing shows that even the currently applied smart metering (SM) technology has a number of drawbacks. Current communication technologies have been shown to exhibit considerable delays and fail to achieve high reliability [4,5,20]. Another quite restricting bottleneck is the non-unified sorting of data that were measured from individual phases. It cannot be assumed that all measured data are correctly assigned to reference phases of power system [21].

The problem of non-unified phase allocation can be addressed by one of the following three methods. The easiest is by proper documentation of all changes to distribution system connection by maintenance personnel. Another one, although costly, is by using special per phase signal injection and receiver devices [22,23] that can match the non-unified phases with reference ones based on the phase with injected signal. The last method is by post-analysis of measured data and finding some type of correlation between series of measurement with non-unified phases and reference measurement [21,24–30].

All of the aforementioned aspects also apply to the case of monitoring of individual MV/LV distribution transformer stations (DTS), which are equipped with power quality (PQ) monitors (analyzers with PQM) by distribution system operators (DSO). Thus, this article is focused on preliminary analysis of bulk measurement of all DTSs in the distribution grid of Brno-stred, that is expected to be pilot project of transition of this extensive traditional urban distribution network towards the smart grid. The analysis is focused on finding the usability and suitability of long term measured data (half year 06/2016–02/2017) from the LV side of all 82 transformers supplying the whole LV distribution system (DS) of the Brno-stred dense mesh with more than 3800 customers. The analysis was primarily focused on finding statistically significant operating states that will be used and helpful for future per phase modelling of this LV network. As the problem with non-unified phases was also identified during the analysis, it was also addressed in this study. The analysis of DS Brno-stred is also unique due to the fact that the LV network is operated as a dense mesh urban network to increase the reliability [12]. As this type of operation might not be so common, not many publications were published dealing with dense mesh networks. Publications [6,9] state that, due to the transition to smart grids, the urban dense mesh networks might need more attention to identify their strong and weak points in the context of changes of these old traditional networks towards bidirectional power flow grids with a high penetration of renewable sources.

The per phase statistical analysis might be helpful for the estimation of load model parameters and forecasting future loading. For example, paper [31] used F-statistic to obtain the load model as a function of voltage and frequency while using data from phasor measurement units. Other researches [32] presented a simple histograms of three years historical data to analyze the correlation between power and voltage changes. Another papers [33–35] used significant statistical values, i.e., mean, median, standard deviation (SD), percentiles (5, 95, 99 etc.), of historical measured data for the estimation of load parameters as well as for evaluation of load forecasting. Gaussian mixed model is also a very powerful statistical approach for the estimation of loads. Its application on historical data was presented in [36–38]. In [39], the loads were modelled by normal and log normal distribution function with division for each of seven days within week. As the input to the load modelling the researchers used usually only summed 3-phase active power values, bulk frequency, phase to phase voltage, and current. Very few or almost none of the researchers dealt with modelling of reactive power loading as well as conducting analysis on per phase basis. Thus, the statistical analysis is done in this paper for the active and reactive power values for each phase separately in the view of dense mesh network (i.e., analysis for all transformers at the global level and also for most (T47) and the least (T61) loaded transformers for different time intervals during days).

2. PQ Monitor Measured Data Processing

The main function of the PQ monitor is to record voltage and current in a three-phase system (L1, L2, L3). The instantaneous values of the voltage and current in regular time intervals might be given by the sampling rate that is an integer multiple (e.g., 32) of the system frequency/period ($T_s = 20$ ms). In the context of monitoring power quality based on [40,41], in a three-phase system the rms values

of voltage and current for each phase in measuring time interval (T_m = 200 ms) are obtained by the following equations

$$U_{x,\text{rms}} = \sqrt{\frac{1}{N}\sum_{n=1}^{N} u_x^2(n)}, \tag{1}$$

where $U_{x,\text{rms}}$ is the rms voltage value in the phase x (i.e., 1, 2 or 3), N is the total number of measured samples, n is a serial number, and $u_x(n)$ is the data sequence of the instantaneous phase values of the sampled voltage waveform.

$$I_{x,\text{rms}} = \sqrt{\frac{1}{N}\sum_{n=1}^{N} i_x^2(n)}, \tag{2}$$

where $I_{x,\text{rms}}$ is the rms value of the current and $i_x(n)$ is the data sequence of the instantaneous phase values of the sampled current waveform.

The apparent power for each phase is evaluated from Equations (1) and (2) at a given moment, being measured over a given time interval (i.e., T_m)

$$S_x = U_{x,\text{rms}} \cdot I_{x,\text{rms}} \tag{3}$$

Furthermore, the active power for each phase is defined as

$$P_x = \frac{1}{N}\sum_{n=1}^{N} u_x(n) \cdot i_x(n) \tag{4}$$

The measurement of reactive energy, as implemented by the manufacturers, generally varies. The problem here might also be caused by the varied definition of reactive power. Usually, it is either the reactive component of power at the fundamental harmonic frequency, which is preferred by the standards, or it is defined by the sum of all reactive powers at the finite number of harmonic frequencies, or it can be calculated including the deformation power as

$$Q_x = \sqrt{S_x^2 - P_x^2} \tag{5}$$

These active and reactive powers/energy flows are further sorted as per four quadrants (Q1–Q4) by [42], with the voltage at the measuring point being taken as the reference vector with zero phase angle. Reactive energy is always defined in association with active energy. Thus, the reactive energy is separately defined for each quadrant. Figure 1 shows the power flow quadrants.
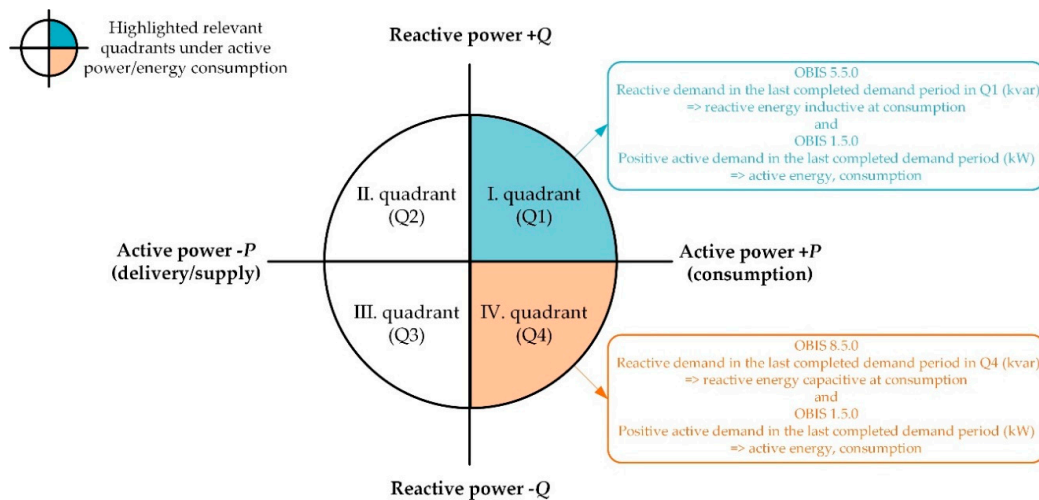

Figure 1. The power flow quadrants and relevant Object Identification System (OBIS) codes.

In general, PQ monitors measure and evaluate a lot of quantities. Thus, the unique marking of the measured quantities (e.g., aggregated active and reactive powers) is accomplished with the use of the DLMS standard [43], through Object Identification System (OBIS) codes, which are a part of the COSEM specifications and some of them are transferred to IEC standards, also see Figure 1.

From the power quality monitoring point of view based on [40], it is also necessary to consider standard aggregation interval for PQ monitors as $N = 10$ min. Thus, the time aggregation of the voltage can be also defined with respecting [41]

$$U_{x,agr} = \sqrt{\frac{1}{N} \sum_{n=1}^{N} U_{x,\mathrm{rms}}^2(n)} \tag{6}$$

The aggregated value of the current is determined in the same way.

In the case of the short-term voltage drop event, Equation (1) is applied over measuring time interval $T_\mathrm{s}/2 = 10$ ms. The obtained $U_{x,\mathrm{rms}/2}$ for each phase is compared with the limits 90% of the nominal voltage according to [40]. Thus, it can be considered that the beginning and ending time of this event are recorded with the maximal inaccuracy 10 ms.

3. Analyzed Distribution Network and Reference Definition

3.1. Dense-Mesh Distribution Network Characteristics

Lots of low voltage (LV) municipal distribution systems in the Czech Republic were formerly often operated with dense-mesh topology. Figure 2 illustrates the general concept of the municipal dense-mesh network that was connected to the individual transformers and distribution transformer stations, respectively.
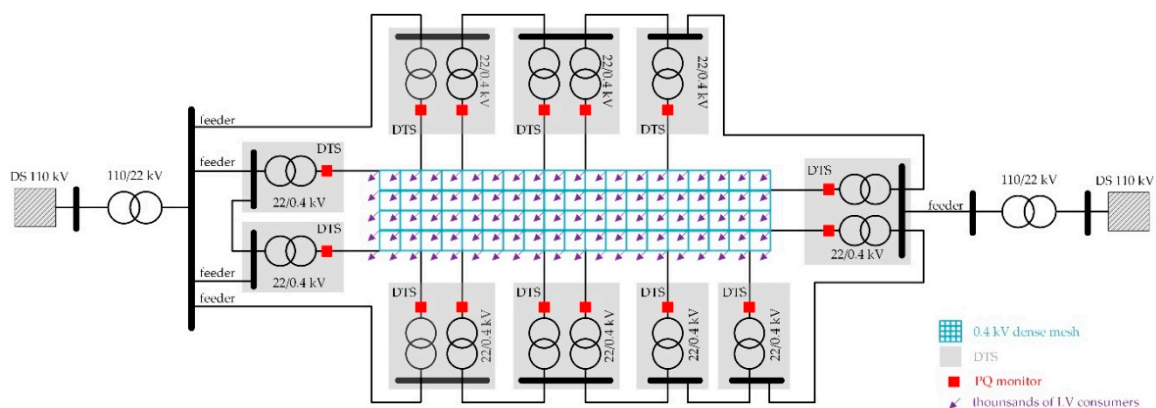

Figure 2. Illustration of the connection concept of the municipal low voltage (LV) dense-mesh distribution system to individual distribution transformation stations and the feeders.

From Figure 2, a high degree of complexity of dense-mesh connections is also visible. Therefore, distribution systems using this concept are usually only operated under test operation in the Czech Republic. The test operation is generally required due to a high number of failures, poor automation of these networks, and their insufficient monitoring. These problems in most cases led to the reconfiguration of the dense-mesh topology to a radial one. Almost all originally dense-mesh distribution systems are operated as with radial topology and they do not allow, technically, the automated reconfiguration back to the dense-mesh ones in general. However, there are still two distribution systems in the Czech Republic that operated as the dense-mesh. One of them, also the largest one, is the Brno-stred, which is analyzed in this paper.

The city planning and technical development of the city of Brno are closely connected and they correspond with its electric energy demands. Thus, the development has direct influence on the

municipal distribution network structure and it also affects the composition of the connected power sources. Due to its size, Brno is divided into individual districts, with each having different distribution network topology, which takes the location of the district into account and also follows its main infrastructure (e.g., industry, transport, municipal council, hospitals, administrative, financial, and educational institutions). The Brno-stred district has a LV distribution network with a dense-mesh topology. Figure 3 shows the complexity of the power supply of this dense-mesh topology by individual feeders and transformers.
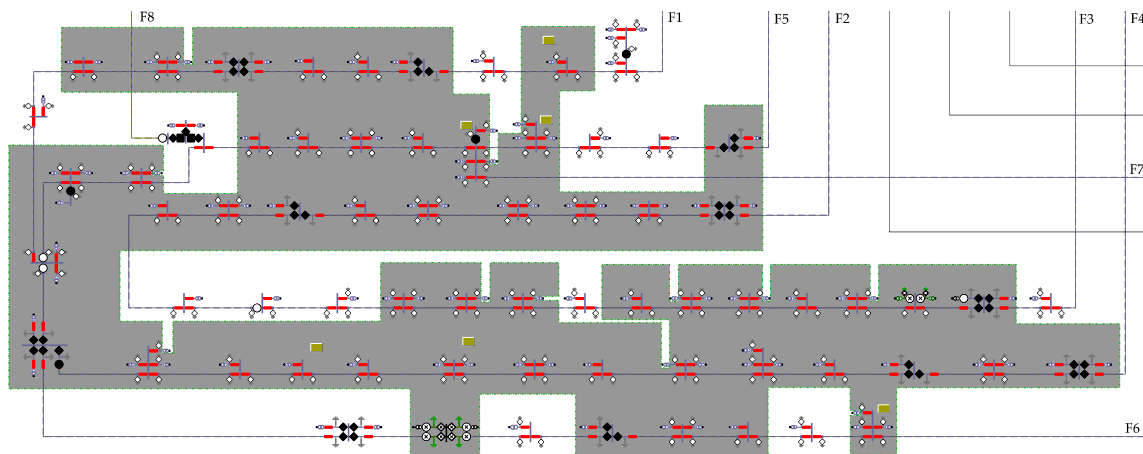
Figure 3. Detail connection of the 56 distribution transformation stations (grey highlighted) of the Brno-stred dense-mesh municipal network.

The Brno-stred distribution system (DS) comprises of 82 transformers 22/0.4 kV, each with an apparent power of 630 kVA with Dyn connection. The total installed power of the transformers is approximately 51.66 MVA. Transformers are located in 56 DTS and they provide power supply to more than 3800 customers connected in the LV 0.4 kV dense mesh. The DS supply is provided by eight 22 kV feeders, marked F1, F2, through to F8. PQ monitors are always installed in the secondary circuit of each transformer and they both have usual synchronization of the internal time by the oscillator frequency and synchronization of the internal time through the network voltage frequency. The analyzed data were anonymized because the municipal distribution network is a part of the critical electricity/energy infrastructure (e.g., transformers T1–T82 assigned randomly inconsistent with marking established by DSO, the manufacturer and model of PQ monitors are not mentioned). Table 1 shows numbers of transformers and DTSs, connected to the feeders F1–F6.

Table 1. Numbers of transformers and distribution transformer stations connected to feeders.

Number of Elements / Feeders	F1	F2	F3	F4	F5	F6
Number of T	11	14	13	19	13	10
Number of DTS	8	9	10	13	9	6

The feeders F1 to F6 are connected to a 110/22 kV (40 MVA) substation through the MV cable and they provide a permanent power supply of the Brno-stred dense-mesh network. Feeders F7 and F8 are connected in case one of F1–F6 is out of service due to a fault or maintenance.

It is very difficult to depict the technical LV scheme clearly in more detail due to the significant extensiveness and the complexity of LV dense-mesh topology. Moreover, it is not required for the initial analysis of power flows at a level of individual transformers. On the other hand, it is necessary to understand that just dense-mesh topology is very unique and specific one, e.g., see Figure 2, and it also has a fundamental impact on the power flows. Thus, achieved results are not directly comparable with the results for radial topology, because there are more complex interdependencies.

3.2. Input Data and Reference Definition

E.ON Distribuce a.s. provided data from PQ monitors comprising of rms voltage, rms current, and average powers for each phase measured with 5 min. intervals between 06/2016 and 02/2017. A three-phase summary value was also recorded in the case of measured powers. The provided data of the powers are not sorted in the individual record interval/measuring time interval, as is generally considered in Figure 1 and (1) through (5), but only one summed average active/reactive power value over all energy quadrants is available in each 5 min. interval (i.e., 5 min. measuring time interval). Therefore, if there were changes in the direction/character of active/reactive power during this 5 min. interval, the measured data are distorted by the significant effect of averaging. Generally, it must be realized that the algorithm itself implemented to measure active/reactive power might essentially have an impact on the attained results. The installed PQ monitors also consider reactive power to be a complement of active power to calculate the apparent power as (5). With regard to the power flow directions (see Figure 1), the data from the installed PQ monitors apply the so-called customer reference arrow system with a reference direction from the HV system to the LV system, see Figure 4.
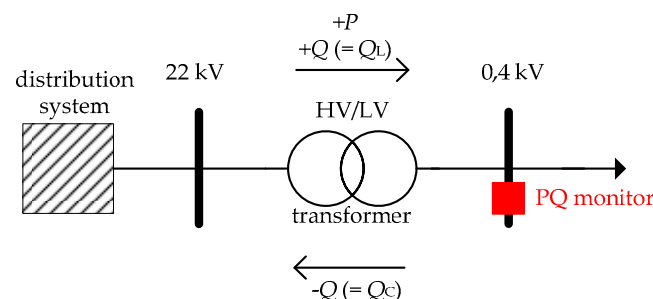
Figure 4. Definition of the reference power flow direction and the location of PQ monitors.

3.3. Conducted Analysis

The measurement data from all transformers from the Brno-stred dense mesh was statistically analyzed for finding statistically significant operating states. Although, the available measurement data was from the period from 06/2016 until 02/2017 for all 82 transformers, it was found out that quite comprehensive analysis can be done only for 56 transformers from time period 01/2017 due to occurrence of various flaws in the data. The complete data were only available for this 56 transformers T1–T14, T16–T54, and T60–T62, and only during 01/2017. Complete data represent 288 records/day/transformer, i.e., 8928 records of 5 min. aggregated values are available for each transformer, specifically 6336 records for the weekdays and 2592 records for the weekends. The various flaws occurring in the rest of the measurement data made the analysis of them impossible, and thus the rest of the data were excluded from the analysis. The possible flaws were as follows: (i) incomplete data, (ii) invalid time vector, and (iii) corrupt data file etc.

In the conducted statistical analysis, the following analyses were conducted, as described in Sections 4.1–4.4:

- Total three-phase and non-unified single phase active and reactive power loading of all 56 transformers during 01/2017.
- Non-unified phase voltage magnitudes and limits of all 56 transformers during 01/2017.
- The power loading of transformer with minimum T61 and maximum T47 power loading was further analyzed in more detail without unified phases for shorter time periods during different part of the weeks. In the analyses, the power loading of both transformers were analyzed with the help of statistical percentiles, minimum, maximum, mean, and standard deviation values.
- The unification of phase measurement of all transformers.

For the unification were used recorded voltage events by PQ monitors. By default, the PQ monitor enables the recording of the voltage events (i.e., the short-term voltage drop in any phase) based on [40]. With regard to the voltage, nine short-term voltage drops (two times in three phases, seven times in two phases) were recorded through PQ monitors for T1–T62 in the period 06/2016–02/2017. The short-term voltage drop records include the initial drop time, drop duration, and the minimum effective voltage and current values in each phase.

4. Results

4.1. Power Loading-Over All Transformers

The basic criterion that was applied by E.ON Distribuce a.s. on the dense-mesh network while it is under operation consists in keeping the loads of the individual transformers within exactly defined limits. Meeting the criterion then leads to ensuring the correct and reliable functioning of the network as a whole. This basic criterion results from the design of the complex topology and size of the network, as well as the fact that it was not possible in the past to implement extensive and efficient ("smart") monitoring of this network. The criterion is mainly based on the ability to ensure a certain extent of autonomous reliability of the network. Autonomous reliability consists in ensuring uninterrupted dense-mesh network operation, even if several transformers fail. The network concept ensures the ability of unaffected transformers to take over the load of the faulted transformers. The DSO requires an operating load of the individual transformers of about 25% in a steady state, or for the maximum power load to ideally not exceed 50% of the transformer rated power, for the proper functioning of the network as a whole.

Thus, the fulfilment of this criterion is assessed in the first part of the analysis, where maximum and minimum power loading of each of 56 transformers (i.e., T1–T14, T16–T54, and T60–T62) was identified. This analysis was only conducted for time period of 01/2017, where complete date for all 56 transformers were available (Section 3.3). The power loads were determined as the sum of the power loads of the individual phases. Figure 5 illustrates the reached maximum power load of individual transformers.
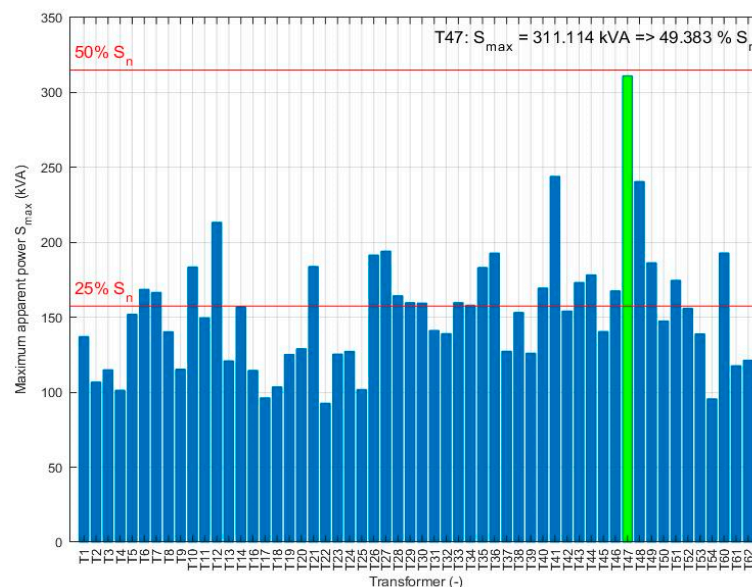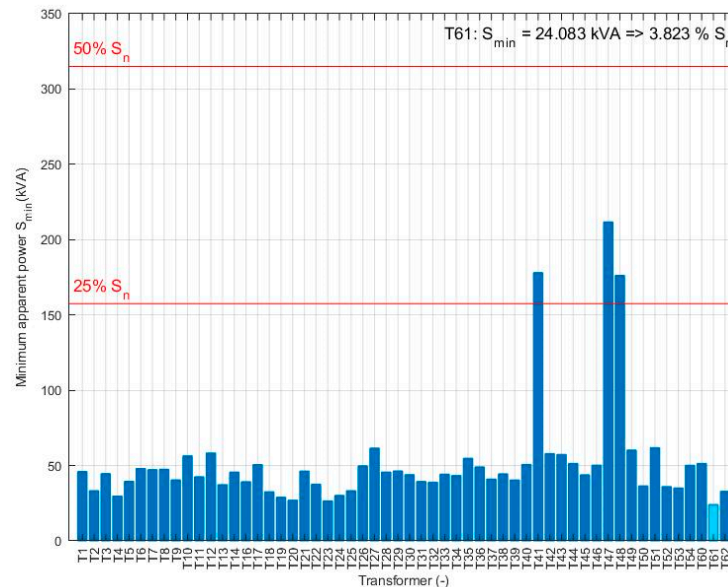

Figure 5. Comparison of the maximum power loads of individual transformers-01/2017.

Figure 5 shows that the maximum power load of approximately 311 kVA (more than 49% S_n) is reached by transformer T47. A total of 32 transformers have the maximum power load below 25% S_n and 23 transformers are in the range (25–40%) S_n. The operating criterion of this DS can be considered

to be fulfilled, as the maximums are not higher than 50% S_n based on analyzed 5 min. data. However, it should be noted that the DSO does not exactly specify the technical requirements for performing the measurement based on which fulfillment of the criterion should be verified. Figure 6 shows the minimum power load to illustrate the opposite extreme loading of individual transformers.


Figure 6. Comparison of the minimum power loads of the individual transformers-01/2017.

The minimum power load of approx. 24 kVA (i.e., approx. 3.8% S_n) is recorded for transformer T61. The values indicate that most transformers do not exceed the level of 50 kVA (approx. 8% S_n).

As the results above provide only a basic picture of the possible extreme operating conditions, the information needs to be understood in the context of averaging over the used 5 min. aggregation interval and further averaged over the three phases as only one value. Therefore, the analysis also includes the statistical evaluation of the magnitudes, together with power flow direction (see also reference direction in Figure 1) of the active and reactive powers in the secondary circuit of each transformer. Figure 6 shows the development of the measured cumulative frequencies of the active and the reactive powers of all analyzed transformers. The single-phase power load data were mixed together for all three phases and Figure 7 depicts cumulative frequencies over all three phases without distinction between separate phases to obtain the cumulative frequencies (single phase data are depicted, not summed powers for all three phases). For a better understanding of the occurrence of the active and the reactive power, it also shows the values separately for the Weekdays and the Weekend, and it is generally proceeded 3×8928 records/month/transformer.

Figure 7 shows that only the consumed active power, approximately 5–84 kW, was realized on transformers and the supplied active power was not realized (for the monitored period 01/2017). Approximately 75% of all active powers ranged up to 40 kW on Weekdays and up to 28 kW during Weekends. From the reactive power point of view, the consumption of approximately (0–71) kvar and the supply of approximately (−18–0) kvar were both realized. It also applies to the reactive power values that the ratio of values for the supplied and consumed reactive power is 40/60 for the Weekdays and 50/50 for the Weekend. Approx. 80% of all values of the supplied reactive power ranged from −18 kvar to −9 kvar (on the Weekdays and on the Weekend) and 90% of all values of the consumed reactive power ranged from 0 kvar to 20 kvar (on the Weekdays) and to approximately 10 kvar (on the Weekend).
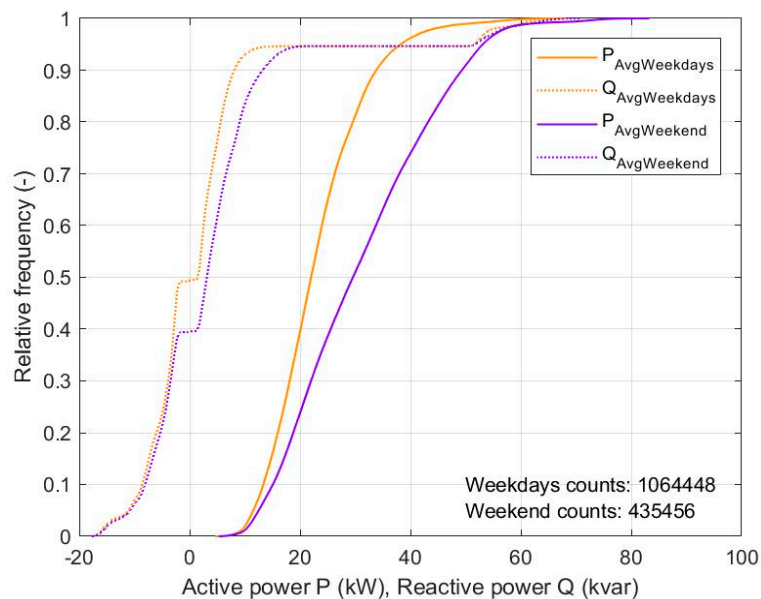
Figure 7. Comparison of the cumulative frequencies of the single-phase active and reactive power of 56 transformers-Weekdays vs. Weekend, 01/2017.

Although there were clearly identified the specific directions of the active and reactive power/energy flows at LV (i.e., consumption vs. supply), it is necessary to point out that all of the installed transformers (i.e., T1–T82) have Dyn connection, and thus the directions need not to explicitly correspond to the power flow directions at HV. With regard to the dense-mesh topology, theoretically plausible explanations for the single-phase supply of the active power may be e.g., (i) the unique configuration and non-symmetrical load character with a significant effect on the size and voltage angle of individual transformers, (ii) failure states on 22 kV side and blowing of one HV fuse, and (iii) operating condition while considering the existence of an unsuitable configuration, where power also flows over this dense-mesh network rather than through the HV network.

Generally, Figure 7 entails the loss of information regarding the possible concurrence of consumption and supply at the level of individual phases of all transformers, because the unified connection of phase measurement does not exist there.

4.2. Voltage Magnitude Distribution Analysis

The kind of complementary analysis that was carried out in this paper is voltage tolerance analysis. The measurement data were evaluated for compliance with voltage tolerance limits of +10% and −15% U_n for 100% of time [40] for 'all' 56 transformers in the Brno-stred dense mesh. The non-unified phase measurement might not be a problem here, as this information regarding voltage compliance can still be found in the available data. Figure 8 shows the histograms of the individual rms phase voltages of 56 transformers without considering the unification of their phase measurements. (i.e., the single-phase histogram was constructed over voltage measurement data from denoted phase one from all transformers together, etc.). The histogram data samples are divided into 50 bins.

The analysis is performed over samples of the individual phase voltages of all transformers, which amounts to 1,064,448 samples for the Weekdays (i.e., 6336 records/phase/transformer/month) and 435,456 samples for weekends (i.e., 2592 records/phase/transformer/month). The values show that all rms voltage values are within the required voltage tolerance [40] during the Weekdays and Weekend. Although the voltage tolerance should be assessed on 10 min. aggregation interval, the eventual reaggregation of 5 min. samples to average 10 min. values would only smoothen the voltage waveform and thus the voltage tolerance would be still met. The problem of non-unified phases

between different measurements might lead to problems in identifying which particular phase is voltage tolerance compliant or non-compliant.
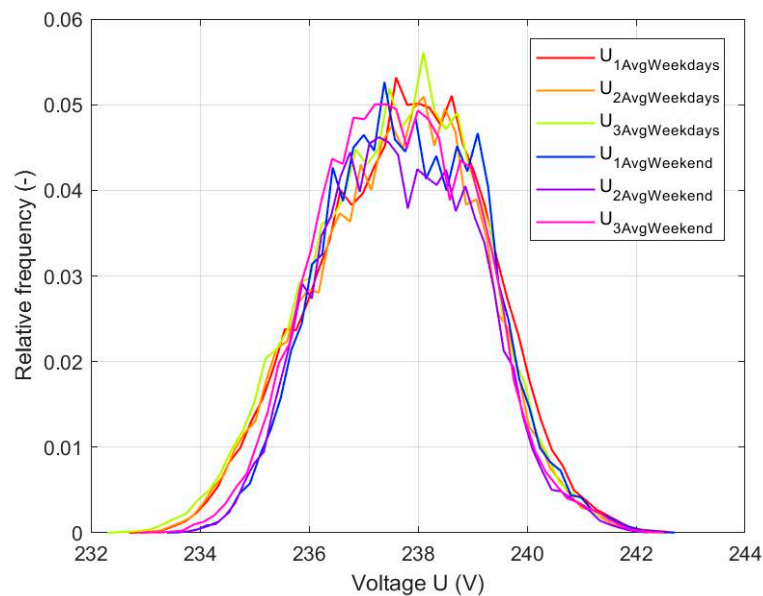
Figure 8. Comparison of relative frequencies of phase voltages of 56 transformers-Weekdays vs. Weekend, 01/2017.

4.3. Transformers with the Maximal T47 and Minimal Power Load T61

Although the unified measurement is not resolved, it is relevant to carry out the partial analysis of individual transformers per each individual phase for 01/2017. A detailed picture can thus be obtained while using percentiles (PCTL) of the occurrence frequencies of power values during the day. In the context of the information above, the article further provides a detailed assessment of the active and reactive power through percentiles/histograms, in particular it presents individual assessments for T47 and T61 differentiating the Weekdays vs. the Weekend.

4.3.1. T47 and T61 Not Sorted Active and Reactive Power to Quadrants

Firstly, Figure 9 shows an overview of the development of the relative frequencies of three-phase apparent power for T47 (with maximum power load) and at T61 (with minimum power load).
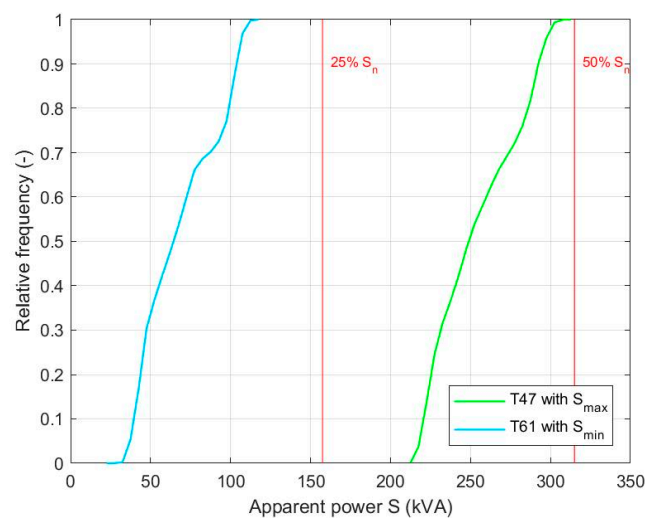
Figure 9. Comparison of relative frequencies of three-phase apparent power for T47 and T61-01/2017.

The histograms show that, for T47, all of the values ranged from 33–49% S_n, approximately 90% of all values were then below 46% of the nominal apparent transformer power. For T61, approximately 70% of all values were below 12% of the nominal apparent power of the transformer and the maximum power did not exceeded 20%. In general, if different energy flows/powers (consumption vs. supply) are simultaneously realized per individual phases, the average three-phase value is unsuitable and it entails a loss of information and lower energy/power is obtained. Thus, Tables 2 and 3 quantify the corresponding percentiles for Figures 10 and 11, which present an overall comparison of cumulative frequencies of the active and reactive power per phase for T47 and T61.
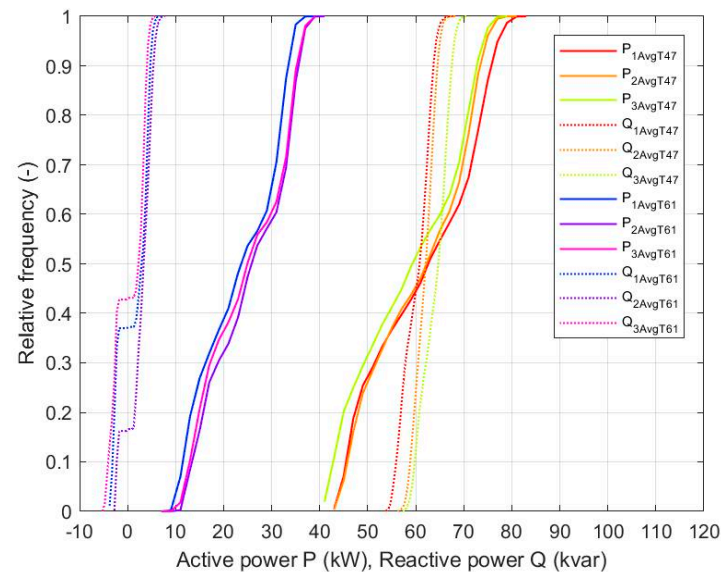
Figure 10. Cumulative frequencies of the single-phase active and reactive power for T47 and T61 during the Weekdays-01/2017.
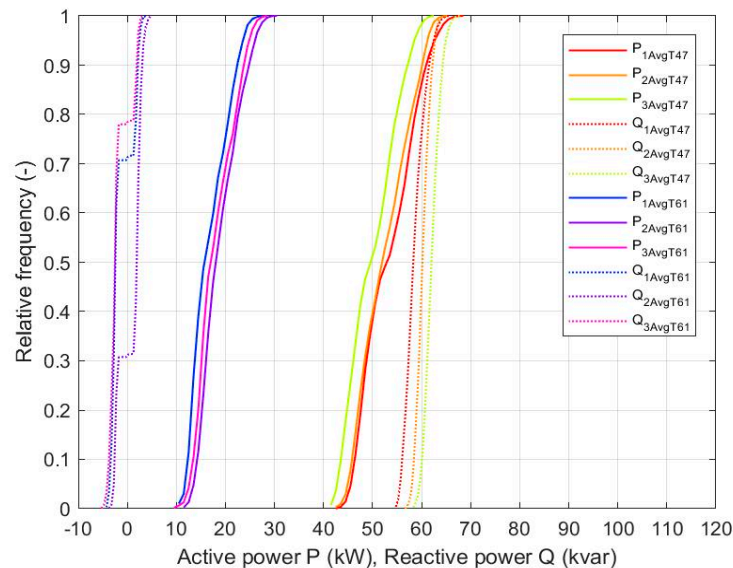
Figure 11. Cumulative frequencies of the single-phase average active and reactive power for T47 and T61 during the Weekend-01/2017.

Table 2. Percentiles of the single-phase active and reactive power for T47 during the Weekdays and the Weekend-01/2017.

Parts of the Week	PCTL	$P_{1AvgT47}$ (kW)	$P_{2AvgT47}$ (kW)	$P_{3AvgT47}$ (kW)	$Q_{1AvgT47}$ (kvar)	$Q_{2AvgT47}$ (kvar)	$Q_{3AvgT47}$ (kvar)
Weekend	50th	53.45	52.4	50.15	58.55	60.31	62.25
	90th	61.44	60.61	57.61	61.8	62.38	64.52
Weekdays	50th	63.6	63.2	60.45	61.05	62.33	64.94
	90th	76.68	74.37	73.74	63.93	64.74	67.75

Table 3. Percentiles of the single-phase active and reactive power for T61 during the Weekdays and the Weekend-01/2017.

Parts of the Week	PCTL	$P_{1AvgT61}$ (kW)	$P_{2AvgT61}$ (kW)	$P_{3AvgT61}$ (kW)	$Q_{1AvgT61}$ (kvar)	$Q_{2AvgT61}$ (kvar)	$Q_{3AvgT61}$ (kvar)
Weekend	50th	16.23	18.55	17.38	−2.19	2.15	−2.3
	90th	22.91	25.3	24.29	2.36	3.22	2.14
Weekdays	50th	24.56	26.64	25.93	3.22	3.58	2.51
	90th	34.33	36.39	36.1	4.98	5.61	4.24

The results in Table 2 prove following:

- in terms of the active power, phase L1 had the highest load and phase L3 the lowest, both during the Weekend and on the Weekdays. On average, the load on the Weekdays was approximately 20% higher than during the Weekend (for 90th PTCL);

- in terms of reactive power, phase L3 had the highest load and phase L1 the lowest, both during the Weekend and on the Weekdays. On average, the loading on the Weekdays was approximately 4% higher than during the Weekend (for 90th PTCL); and,

- the comparison of percentiles in individual phases indicates that the power distribution in the individual phases is relatively even, with 90th and 50th PTCLs differing in individual phases by only about 3–4 kW, for both the analyzed Weekdays and Weekend periods (i.e., for example the difference for the 90th PTCL on the Weekdays-the largest L1 ~61.44 kW, and the smallest L3 57.61 kW difference of about 4 kW). As for reactive power, the difference was similar in size to the active power of about 3–4 kvar. The reactive power was comparable in size to the active power.

The results in Table 3 prove the following:

- in terms of the consumed active power, phase L2 had the highest load and phase L1 the lowest, both during the Weekdays and the Weekend. On average, the load on the Weekdays was approximately 32% higher than during the Weekend (for 90th PTCL); and,

- if the transformer provides the consumption as well as the supply of the reactive power in the monitored period and the analyzed data are not divided according to the power character (i.e., the data series cumulates all of the consumed/supplied reactive powers), and then the evaluation of the reached reactive power through percentiles is not representative.

In general, the results in Table 3 also confirm that, in order to do the basic statistical evaluation of the transformer that provides the consumption of the active power and at the same time the consumption or the supply of the reactive power, it is firstly appropriate to sort the data based on the character of the reactive power.

4.3.2. T47 and T61 Sorted Active and Reactive Powers to Quadrants and Their Statistical Values

Sorting is separately performed for each phase in the context of quadrants Q1 and Q4, as in Figure 1. Thus, the following Table 4 provides this sorting by presenting a percentage of the numbers

of single-phase reactive power records, with both the differentiation between the Weekdays vs. Weekend and the distribution considering four time-periods during the day A (22:00:00–03:59:59), B (4:00:00–07:59:59), C (08:00:00–15:59:59), and D (16:00:00–21:59:59).

Table 4. Percentages of the numbers of single-phase reactive power records for T61 sorted by–consumed Q ($Q > 0$), supplied Q ($Q < 0$), no Q ($Q = 0$), red text highlights dominant one per phase.

Parts of the Week	Time Interval	Number of Records	$Q_{1AvgT61}$			$Q_{2AvgT61}$			$Q_{3AvgT61}$		
			>0 (%)	<0 (%)	=0 (%)	>0 (%)	<0 (%)	=0 (%)	>0 (%)	<0 (%)	=0 (%)
Weekend	A	648	18.7	79.9	1.4	84.7	15.1	0.2	8	91.4	0.6
	B	432	33.8	64.6	1.6	77.8	21.1	1.2	33.1	65.5	1.4
	C	864	13.3	86.5	0.2	35.3	64.1	0.6	7.4	92.5	0.1
	D	648	54.5	44.6	0.9	91	8.5	0.5	45.1	53.7	1.2
Weekdays	A	1584	5.4	94.1	0.4	40.9	58.3	0.8	0.9	98.9	0.2
	B	1056	55.3	44.4	0.3	89	9.8	1.1	45.8	53.6	0.6
	C	2112	100	0	0	100	0	0	99.1	0.7	0.1
	D	1584	75.4	24.2	0.4	99.9	0.1	0	63.8	35.6	0.6

The sorting for T47 is irrelevant, because there is no change of the character of the reactive power (i.e., only Q consumption, 100% of the records fulfill condition $Q > 0$), therefore there are the results for T61 in Table 4, and these show:

- during the Weekend/A and Weekend/B, the number of records corresponding to the supplied reactive power predominates in phases L1 and L3, and the consumed reactive power predominates in phase L2;
- during the Weekend/D and Weekdays/B the number of records of the consumed reactive power significantly predominates in L2, while in L1 and L2 the balance of represented samples is leveled;
- during the Weekend/C and Weekdays/A the number of records of the supplied reactive power predominates in all phases; and,
- significant and predominating reactive power character (the consumption or the supply) is identifiable per phase for each specific time intervals during the day in individual parts of the week, e.g., solely the supplied reactive power is identified for T61 during the Weekdays/C period in phases L1 and L2, and it is also almost 100% in phase L3. A similar and also strong dependence is also observed in the Weekdays/D.

The data also generally include the values that stand for zero reactive power (see Table 4). However, these were not considered further in the statistical evaluation due to their percentage being insignificant.

The following Tables 5–7 present a summary statistical analysis by the percentiles. Specifically, for T61, Tables 6 and 7 present the percentile results performed on the sorted samples according to Table 4. The data were initially sorted according to the character of the reactive power into two groups for consumed Q (quadrant Q1) and supplied Q (quadrant Q4) to determine the percentiles. In this sorting, the corresponding active power samples P were also sorted for the corresponding Q samples. Over such sorted data, the percentiles were subsequently set separately for the active power (for given character of the reactive power) and for the reactive power.

Table 5. Percentiles of the single-phase active power and reactive power at the time of the reactive power consumption for T47-01/2017.

Parts of the Week	Time Interval	PCTL	$P_{1AvgT47}$ (kW)	$P_{2AvgT47}$ (kW)	$P_{3AvgT47}$ (kW)	$Q_{1AvgT47}$ (kvar)	$Q_{2AvgT47}$ (kvar)	$Q_{3AvgT47}$ (kvar)
Weekend	A	5th	46.70	47.35	43.60	56.85	59.02	60.38
		25th	48.41	49.09	45.45	57.76	59.94	61.24
		50th	50.09	50.76	47.01	58.41	60.59	62.06
		75th	51.96	52.43	48.95	59.38	61.37	63.10
		90th	54.41	54.98	50.99	60.61	62.13	64.22
	B	5th	45.05	44.45	42.15	55.61	57.42	58.94
		25th	46.29	45.62	43.42	56.33	58.62	59.91
		50th	47.36	46.50	44.34	56.93	59.25	60.72
		75th	48.30	47.33	45.50	57.65	59.82	61.40
		90th	49.27	48.15	46.60	58.16	60.31	62.14
	C	5th	46.70	45.56	44.82	55.60	58.15	60.20
		25th	52.03	49.86	49.09	57.30	59.23	61.61
		50th	57.09	54.65	53.34	58.63	60.15	62.35
		75th	60.31	59.34	56.53	59.80	61.01	63.20
		90th	62.66	61.21	59.15	60.94	61.74	64.11
	D	5th	50.06	48.84	47.27	56.16	58.39	60.84
		25th	56.15	55.41	52.74	59.08	60.24	62.46
		50th	58.13	57.47	54.41	60.64	61.47	63.63
		75th	60.26	59.99	56.45	62.10	62.40	64.59
		90th	62.86	61.77	58.43	63.34	63.13	65.76
Weekdays	A	5th	44.75	45.19	41.94	55.52	58.56	59.33
		25th	46.56	47.21	44.05	56.81	59.63	60.39
		50th	48.10	49.19	45.93	57.62	60.35	61.32
		75th	51.73	52.94	49.46	58.78	61.18	62.87
		90th	54.94	55.76	52.43	60.19	61.94	64.03
	B	5th	44.88	44.93	42.26	54.82	57.69	58.49
		25th	46.57	46.27	43.57	55.61	58.64	59.69
		50th	49.66	48.89	47.77	56.48	59.29	60.55
		75th	55.02	54.12	53.17	57.49	60.30	62.28
		90th	58.87	56.93	55.98	58.58	61.33	63.44
	C	5th	65.63	63.86	63.18	59.46	61.62	64.34
		25th	72.97	70.86	70.27	61.39	62.91	65.85
		50th	75.00	72.80	72.26	62.46	63.73	66.71
		75th	76.99	74.62	74.05	63.46	64.54	67.56
		90th	78.76	76.19	75.59	64.25	65.22	68.22
	D	5th	58.54	59.23	55.70	59.94	61.16	63.24
		25th	62.83	62.96	59.44	61.74	62.36	64.99
		50th	67.07	66.08	63.41	62.77	63.32	65.98
		75th	71.48	70.24	68.56	63.69	64.20	66.94
		90th	73.74	72.29	70.89	64.63	65.06	68.11

Table 6. Percentiles of the single-phase active power and reactive power at the time of the reactive power consumption for T61-01/2017.

Parts of the Week	Time Interval	PCTL	$P_{1AvgT61}$ (kW)	$P_{2AvgT61}$ (kW)	$P_{3AvgT61}$ (kW)	$Q_{1AvgT61}$ (kvar)	$Q_{2AvgT61}$ (kvar)	$Q_{3AvgT61}$ (kvar)
Weekend	A	5th	13.84	13.79	15.34	1.89	1.83	1.79
		25th	14.94	14.99	16.08	2.00	2.16	1.88
		50th	15.93	16.04	17.72	2.09	2.53	1.96
		75th	16.80	17.55	18.79	2.19	2.91	2.06
		90th	18.00	18.93	19.84	2.26	3.22	2.13
	B	5th	12.47	15.59	14.35	1.64	1.61	1.53
		25th	13.25	16.57	15.39	1.74	1.82	1.68
		50th	13.99	17.25	15.96	1.81	2.18	1.79
		75th	15.02	17.95	16.61	1.89	2.75	1.90
		90th	15.44	18.75	17.07	2.00	3.16	2.00
	C	5th	19.18	19.77	21.12	1.91	1.88	1.84
		25th	20.74	21.84	22.64	2.04	2.06	1.97
		50th	22.14	23.14	24.31	2.18	2.19	2.05
		75th	23.67	24.63	25.06	2.41	2.37	2.38
		90th	24.93	25.82	25.82	2.55	2.55	2.69
	D	5th	18.94	19.38	22.00	2.08	2.06	1.95
		25th	21.63	21.57	23.48	2.26	2.39	2.15
		50th	23.14	23.54	24.59	2.45	2.76	2.31
		75th	24.19	26.16	25.86	2.77	3.37	2.50
		90th	25.05	27.54	26.87	3.10	3.96	2.79
Weekdays	A	5th	15.55	13.96	16.89	1.97	1.92	1.95
		25th	17.30	16.13	18.61	2.10	2.10	2.04
		50th	18.63	18.35	19.29	2.26	2.28	2.13
		75th	19.92	20.64	23.02	2.40	2.54	2.24
		90th	20.68	22.00	23.65	2.55	2.97	2.42
	B	5th	14.44	16.33	16.91	1.81	1.61	1.78
		25th	18.29	17.44	19.86	2.84	1.82	2.09
		50th	20.60	21.38	22.11	3.58	2.86	2.55
		75th	23.17	25.00	24.16	4.07	3.56	3.13
		90th	25.11	26.43	25.53	4.60	3.96	3.53
	C	5th	27.59	28.27	27.08	3.54	3.58	2.84
		25th	31.63	33.22	32.97	4.11	4.30	3.34
		50th	33.08	34.93	34.73	4.50	4.80	3.69
		75th	34.39	36.19	35.93	4.91	5.27	4.08
		90th	35.39	37.41	37.16	5.32	5.72	4.45
	D	5th	22.34	23.01	24.79	2.36	2.47	2.22
		25th	25.13	25.56	30.15	2.65	3.09	2.84
		50th	30.20	29.95	33.78	3.65	4.09	3.65
		75th	32.74	35.05	35.56	4.42	5.47	4.25
		90th	34.00	36.44	36.70	5.07	6.21	4.75

Table 7. Percentiles of the single-phase active power and reactive power at the time of the reactive power supply for T61-01/2017.

Parts of the Week	Time Interval	PCTL	$P_{1AvgT61}$ (kW)	$P_{2AvgT61}$ (kW)	$P_{3AvgT61}$ (kW)	$Q_{1AvgT61}$ (kvar)	$Q_{2AvgT61}$ (kvar)	$Q_{3AvgT61}$ (kvar)
Weekend	A	5th	11.81	13.35	12.88	−3.28	−2.53	−4.30
		25th	13.14	14.82	14.33	−2.60	−2.32	−2.78
		50th	13.98	15.61	15.36	−2.25	−2.12	−2.33
		75th	14.90	16.30	16.64	−2.06	−1.99	−2.09
		90th	15.86	17.17	18.18	−1.97	−1.90	−1.95
	B	5th	12.35	14.85	13.31	−2.47	−2.04	−2.58
		25th	12.96	15.50	14.96	−2.20	−1.89	−2.28
		50th	13.48	16.21	15.56	−2.04	−1.78	−2.07
		75th	14.19	16.75	16.06	−1.88	−1.67	−1.85
		90th	14.90	17.70	16.55	−1.78	−1.61	−1.69
	C	5th	11.91	13.00	12.35	−3.65	−2.91	−3.68
		25th	14.96	15.42	15.67	−3.08	−2.45	−3.27
		50th	18.18	18.41	19.01	−2.76	−2.24	−2.91
		75th	20.68	20.49	22.23	−2.44	−2.09	−2.45
		90th	22.11	22.72	23.62	−2.21	−1.96	−2.17
	D	5th	13.76	14.40	14.47	−3.40	−2.39	−4.26
		25th	16.80	15.57	17.99	−2.71	−2.29	−3.18
		50th	18.15	16.58	20.06	−2.43	−2.17	−2.48
		75th	19.77	18.72	21.54	−2.25	−2.09	−2.27
		90th	20.86	19.15	22.71	−2.11	−1.95	−2.12
Weekdays	A	5th	10.74	12.30	11.80	−3.49	−2.39	−4.54
		25th	11.88	13.25	13.31	−3.08	−2.20	−4.10
		50th	12.91	13.99	14.65	−2.78	−2.07	−3.55
		75th	15.30	14.92	16.70	−2.44	−1.97	−2.88
		90th	17.51	16.31	18.98	−2.24	−1.86	−2.41
	B	5th	11.93	12.98	14.03	−2.66	−2.20	−3.57
		25th	13.39	15.37	15.47	−2.21	−1.94	−2.43
		50th	13.99	16.34	16.21	−2.02	−1.78	−2.17
		75th	14.56	16.71	17.04	−1.88	−1.66	−1.99
		90th	15.22	16.98	18.09	−1.79	−1.52	−1.83
	C	5th	0.00	0.00	23.09	0.00	0.00	−3.12
		25th	0.00	0.00	25.08	0.00	0.00	−2.86
		50th	0.00	0.00	26.50	0.00	0.00	−2.60
		75th	0.00	0.00	28.07	0.00	0.00	−2.57
		90th	0.00	0.00	32.20	0.00	0.00	−2.52
	D	5th	19.74	23.14	21.35	−2.77	−2.37	−2.82
		25th	21.47	23.14	23.51	−2.59	−2.37	−2.57
		50th	22.71	23.14	24.85	−2.49	−2.37	−2.42
		75th	23.82	23.14	26.10	−2.38	−2.37	−2.29
		90th	24.70	23.14	26.90	−2.27	−2.37	−2.19

For transformer T47, based on the comparison of 90th PTCL results from Table 2 (only the summary Weekdays and Weekend percentiles are considered) and Table 5 (considers both the summary percentiles and the individual time intervals A, B, C, D during day) can be observed with following dependencies:

- the summary Weekend PCTLs of the single-phase active and reactive power achieved are comparable to those achieved during the Weekend/C and Weekend/D with differences of approximately 1–3%;
- a similar dependence is also observed at the summary Weekdays PCTLs vs. Weekdays/C and Weekdays/D, although these differ by approximately 1–4%;
- for other time intervals A and B it is possible to observed more significant differences against the summary PCTLs

  ○ the summary Weekend PCTLs of the active power are approx. 10% higher than those for the Weekend/A, for the reactive power they are approx. 1–2% higher,

○ the summary Weekend PCTLs of the active power are approx. 20% higher than those for the Weekend/B, for the reactive power they are approx. 4–5% higher,

○ the summary Weekdays PCTLs of the active power are approx. 25–29% higher than those for the Weekdays/A, for the reactive power they are approx. 5% higher, and

○ the summary Weekdays PCTLs of the active power are approx. 24% higher than those for the Weekdays/B, for the reactive power they are approx. 5–8% higher.

Finding the interdependencies for T61 is very complicated, not only for the confrontation summary percentiles (in Table 3) with the results in Tables 6 and 7, but also generally from the individual percentiles in case of the change of the character of reactive power flow. Thus, it would first be necessary to define the specific purpose for which the analysis is to be prioritized (e.g., reactive power flows, voltage magnitude, unbalance, etc.) and it should be performed over the phase unified data of all transformers. On the other hand, the search for basic interdependencies can also be done while using other statistical indicators. Therefore, the following part of the analysis evaluates the values of the maximal and minimal power, the mean and the standard deviation in more detail over the sorted data. Tables 8–10 show the obtained results.

Table 8. Statistical results for T47 at the time of the reactive power consumption including the highlighted total ==maximal== and ==minimal== powers and ==the highest absolute mean values== per phase.

Parts of the Week	Time Interval	Quantity	$P_{1AvgT47}$ (kW)	$P_{2AvgT47}$ (kW)	$P_{3AvgT47}$ (kW)	$Q_{1AvgT47}$ (kvar)	$Q_{2AvgT47}$ (kvar)	$Q_{3AvgT47}$ (kvar)
Weekend	A	Max	60.89	58.75	54.31	63.13	63.97	66.04
		Min	44.79	45.68	41.77	55.67	57.63	59.56
		Mean	50.54	51.02	47.34	58.68	60.67	62.26
		SD	2.93	2.59	2.53	1.41	1.08	1.33
	B	Max	54.48	50.09	49.66	59.39	61.24	63.49
		Min	43.99	42.65	41.46	54.52	56.55	58.15
		Mean	47.39	46.51	44.51	56.98	59.17	60.69
		SD	1.59	1.26	1.59	0.90	0.92	1.08
	C	Max	67.22	63.91	62.63	63.58	64.59	66.40
		Min	42.97	42.17	42.68	54.85	57.00	59.03
		Mean	56.16	54.36	52.94	58.60	60.14	62.38
		SD	5.38	5.37	4.75	1.79	1.24	1.27
	D	Max	68.30	65.14	61.80	65.84	64.71	67.95
		Min	48.13	47.07	45.45	54.99	57.51	59.68
		Mean	57.96	57.17	54.17	60.48	61.25	63.55
		SD	4.00	3.92	3.33	2.28	1.54	1.60
Weekdays	A	Max	61.75	60.63	57.70	63.44	63.70	66.24
		Min	43.22	43.25	40.32	53.92	56.91	58.07
		Mean	49.26	50.10	46.85	57.90	60.42	61.63
		SD	3.73	3.73	3.68	1.65	1.14	1.64
	B	Max	64.31	61.97	62.69	61.27	64.29	66.74
		Min	43.94	43.54	40.92	53.60	56.43	57.35
		Mean	51.09	50.20	48.56	56.66	59.54	60.98
		SD	5.18	4.48	5.24	1.36	1.32	1.77
	C	Max	83.12	80.15	79.53	67.63	67.38	70.21
		Min	58.61	57.61	56.73	56.77	59.36	61.91
		Mean	74.45	72.20	71.63	62.35	63.71	66.64
		SD	3.94	3.75	3.72	1.58	1.21	1.28
	D	Max	80.01	77.56	75.99	67.23	68.40	70.97
		Min	53.80	54.65	52.00	58.22	59.89	61.61
		Mean	67.05	66.44	63.86	62.71	63.30	65.99
		SD	5.24	4.51	5.26	1.51	1.32	1.58

Table 9. Statistical results for T61 at the time of the reactive power consumption, including the highlighted total `maximal` and `minimal` powers and `the highest absolute mean values` per phase.

Parts of the Week	Time Interval	Quantity	$P_{1AvgT61}$ (kW)	$P_{2AvgT61}$ (kW)	$P_{3AvgT61}$ (kW)	$Q_{1AvgT61}$ (kvar)	$Q_{2AvgT61}$ (kvar)	$Q_{3AvgT61}$ (kvar)
Weekend	A	Max	19.52	23.56	21.94	2.52	4.63	2.21
		Min	13.53	12.65	15.04	1.78	1.53	1.76
		Mean	15.98	16.38	17.68	2.10	2.57	1.97
		SD	1.38	1.88	1.75	0.14	0.51	0.12
	B	Max	16.27	20.52	18.18	2.37	3.74	2.30
		Min	12.11	12.37	13.59	1.55	1.39	1.45
		Mean	14.12	17.26	15.94	1.82	2.31	1.80
		SD	1.02	1.13	0.88	0.13	0.57	0.17
	C	Max	26.67	27.87	28.04	3.11	3.45	3.31
		Min	18.09	17.27	20.74	1.82	1.74	1.75
		Mean	22.24	23.12	24.01	2.25	2.23	2.18
		SD	1.91	2.01	1.70	0.27	0.25	0.34
	D	Max	27.61	30.17	28.29	3.93	4.91	3.47
		Min	16.95	16.70	18.12	1.85	1.87	1.58
		Mean	22.82	23.78	24.61	2.55	2.93	2.35
		SD	2.00	2.82	1.76	0.38	0.69	0.29
Weekdays	A	Max	21.51	25.02	24.02	3.05	4.70	2.44
		Min	14.73	12.59	16.87	1.87	1.66	1.95
		Mean	18.58	18.31	20.40	2.27	2.40	2.16
		SD	1.63	2.78	2.49	0.23	0.47	0.15
	B	Max	28.41	29.26	31.06	5.67	5.17	5.63
		Min	13.42	13.51	15.84	1.58	1.41	1.55
		Mean	20.66	21.32	22.02	3.45	2.77	2.66
		SD	3.40	3.93	2.85	0.92	0.93	0.67
	C	Max	38.21	41.54	39.78	6.55	7.81	5.84
		Min	7.61	8.21	7.86	1.68	1.08	1.54
		Mean	32.69	34.40	34.04	4.53	4.80	3.73
		SD	2.57	2.86	3.10	0.63	0.74	0.56
	D	Max	36.87	39.72	39.61	6.77	7.90	5.83
		Min	18.89	20.37	21.94	2.10	1.99	1.84
		Mean	29.21	30.20	32.57	3.66	4.29	3.59
		SD	4.14	5.00	3.97	1.03	1.36	0.89

The results in Table 8 show that T47 has the maximal consumed active and reactive power during the Weekdays approx. 15–17 kW and 2–3 kvar higher than during the Weekend. Furthermore, transformer T47 reaches approximately the same average values of the minimal consumed active and reactive power during the Weekdays and the Weekend.

The results in Table 9 show that the maximal consumed active and reactive power for transformer T61 during the Weekdays is approx. 11 kW and 2.5–3 kvar higher than during the Weekend. The minimal consumed active power during the Weekdays is approx. 4–6 kW lower than during the Weekend and the minimal consumed reactive power is similar for the Weekdays and Weekend.

The results in Table 10 show that the maximal consumed active power for transformer T61 has differences of approx. 3–6 kW and this transformer reaches similar values of the maximal supplied reactive power during the Weekdays and Weekend. This similarity is also observed for the minimal consumed active and supplied reactive power, respectively.

Table 10. Statistical results for T61 at the time of the reactive power supply including the highlighted total <mark style="background:red">maximal</mark> and <mark style="background:yellow">minimal</mark> powers and <mark style="background:green">the highest absolute mean values</mark> per phase.

Parts of the Week	Time Interval	Quantity	$P_{1AvgT61}$ (kW)	$P_{2AvgT61}$ (kW)	$P_{3AvgT61}$ (kW)	$Q_{1AvgT61}$ (kvar)	$Q_{2AvgT61}$ (kvar)	$Q_{3AvgT61}$ (kvar)
Weekend	A	Max	19.03	18.35	21.97	−1.74	−1.74	−1.71
		Min	10.17	12.91	12.05	−3.82	−2.76	−5.07
		Mean	14.08	15.56	15.62	−2.38	−2.16	−2.61
		SD	1.45	1.26	1.88	0.43	0.22	0.75
	B	Max	16.01	18.58	17.44	−1.51	−1.49	−1.49
		Min	10.34	14.19	11.31	−2.71	−2.42	−3.22
		Mean	13.60	16.26	15.42	−2.06	−1.79	−2.08
		SD	0.91	0.95	1.02	0.23	0.16	0.30
	C	Max	24.45	24.53	26.30	−1.81	−1.63	−1.70
		Min	10.12	11.63	9.52	−4.19	−3.53	−4.15
		Mean	17.73	18.10	18.75	−2.79	−2.30	−2.88
		SD	3.39	3.25	3.85	0.47	0.31	0.51
	D	Max	24.59	20.83	26.39	−1.90	−1.81	−1.71
		Min	12.45	14.13	13.05	−3.69	−2.57	−4.70
		Mean	18.12	16.98	19.68	−2.53	−2.18	−2.77
		SD	2.25	1.80	2.67	0.41	0.16	0.70
Weekdays	A	Max	21.11	20.32	23.91	−1.87	−1.56	−1.91
		Min	9.60	11.40	10.26	−3.98	−2.72	−5.19
		Mean	13.68	14.22	15.17	−2.78	−2.08	−3.48
		SD	2.39	1.41	2.54	0.42	0.18	0.72
	B	Max	17.30	17.92	20.12	−1.48	−1.36	−1.50
		Min	10.03	12.22	11.28	−3.69	−2.44	−4.90
		Mean	13.95	15.80	16.26	−2.08	−1.80	−2.29
		SD	1.08	1.38	1.42	0.31	0.22	0.53
	C	Max	0.00	0.00	32.37	0.00	0.00	−2.42
		Min	0.00	0.00	22.88	0.00	0.00	−3.13
		Mean	0.00	0.00	27.18	0.00	0.00	−2.71
		SD	0.00	0.00	2.96	0.00	0.00	0.21
	D	Max	27.41	23.14	28.98	−2.07	−2.37	−1.84
		Min	17.78	23.14	18.61	−2.98	−2.37	−3.73
		Mean	22.62	23.14	24.73	−2.49	−2.37	−2.45
		SD	1.69	0.00	1.82	0.16	0.00	0.22

The general conclusions can be drawn when comparing the results of Tables 8–10:

- the highest mean values for T47 are usually achieved in the Weekdays/C. The minimal differences of approx. 11% are in the comparison with the Weekdays/D, for other interval the differences are roughly 30–35%;
- the highest mean values achieved for T47 during the Weekend are in the Weekend/D but differences with other Weekend intervals are under 18% for the active power and under 6% the reactive power;
- the mean values of the active power for T47 are approx. 14–25% higher in the intervals Weekdays/C and Weekdays/D than those for Weekend/C and Weekend/D, for the reactive power they are similar in all intervals and the most of differences are lower than 6%; and,
- similar dependencies can be found for T61 as for T47, when the values are usually higher during the Weekdays than during the Weekend. Specifically, the active power values during the Weekdays are usually 11–33% higher than those during the Weekend and the reactive power differs in the range 1–54%. Although high percentage differences between corresponding intervals were achieved, it should be noted that, in terms of absolute values, these are comparable to differences for the transformer T47 when these are not higher than 5% and 1% of the nominal power of transformer, e.g., for the active power (10.5 kW/per phase) and the reactive power (2.5 kvar/per phase).

4.4. Unification of Phase Allocation

The authors have demonstrated earlier in [21] the use of the phase identification method on the experimental one-year worth of voltage data from smart meters that were installed in DS with radial

topology. However, the sensitivity of this method is highly dependable on the amount of long-term data and it is better suited for radial topology of distribution network. Therefore, in the case of DS Brno-stred with an extensive dense-mesh topology, a different post processing approach of phase identification from the one that was published in [21] was used. The approach is basically based on the use of recorded voltage events/drops by PQ monitors for T1–T62. Table 11 quantifies these voltage drops in the transformer T1, which is considered as a reference one from the phase identification point of view.

Table 11. Short-term voltage drops in the reference transformer T1-06/2016–02/2017.

Number of the Events	U_{1T1}/U_n (−)	U_{2T1}/U_n (−)	U_{3T1}/U_n (−)	Affected Phases	Status
1	0.878	0.884	0.883	L1-L2-L3	not used
2	0.992	0.759	0.775	L2-L3	used for L1
3	0.995	0.753	0.754	L2-L3	used for L1
4	0.701	0.671	1.016	L1-L2	used for L3
5	0.876	1.014	0.876	L1-L3	used for L2
6	0.725	0.733	0.989	L1-L2	used for L3
7	1.001	0.754	0.683	L2-L3	used for L1
8	0.844	1.002	0.820	L1-L3	used for L2
9	0.878	0.885	0.882	L1-L2-L3	not used

Generally, the short-term voltage drop records include the initial drop time, drop duration, and the minimum effective voltage and current values in each phase. Table 11 shows the three-phase voltage drops that occurred twice and the two-phase voltage drops that occurred seven times. If the short-term voltage drops in one (L1, L2 or L3) or two phases (L1-L2, L1-L3, or L2-L3) are available, it is theoretically possible to use them to unify the measurement phases with reference one in a whole monitored system. In the case of a single-phase voltage drop, this significant drop can also be observed in each one specific phase of transformers. On the other hand, in the case of two-phase voltage drop, the object of observation is the phase without voltage drop. Thus, Table 12 brings the results of the phase identification with the reference T1 while using the mentioned two-phase voltage drop events (i.e., events 2–8 in Table 11) that were recorded by individual PQ monitors.

The results indicate good usability of the short-voltage drop events for the phase identification/unification of the measurement, when the phases were assigned to transformers T1–T59. However, in the case of three transformers (T2, T3, and T42), a reverse phase sequence was assigned. The rest of transformers was assigned a correct phase sequence. The phases of transformers T60–T62 remained unidentified because at the time of the voltage events recorded at T1, the PQ monitors at these transformers have not been installed yet. The results also show the ability to identify the individual phases of the measurement in 100% of the cases when PQ monitors recorded the short-voltage drop events. Specifically, 37 transformers have the same phase measurement position as the reference one. However, it is necessary to verify the results by comparing them with the actual PQ monitors HW connection directly at DTS. As this verification has not been done yet, this article further presents only a detailed analysis over the non-unified data.

Table 12. Results of the phases identification of the measurement–reference T1.

TR No.	Identified Phases			Status	TR No.	Identified Phases			Status
1	L1	L2	L3	reference	32	L1	L2	L3	correct
2	L3	L2	L1	reverse	33	L1	L2	L3	correct
3	L3	L2	L1	reverse	34	L2	L1	L3	correct
4	L3	L1	L2	correct	35	L2	L3	L1	correct
5	L1	L2	L3	correct	36	L1	L2	L3	correct
6	L1	L2	L3	correct	37	L1	L2	L3	correct
7	L1	L2	L3	correct	38	L2	L3	L1	correct
8	L1	L2	L3	correct	39	L1	L2	L3	correct
9	L3	L1	L2	correct	40	L3	L1	L2	correct
10	L2	L1	L3	correct	41	L1	L2	L3	correct
11	L1	L3	L2	correct	42	L3	L2	L1	reverse
12	L1	L2	L3	correct	43	L1	L2	L3	correct
13	L3	L1	L2	correct	44	L1	L2	L3	correct
14	L1	L2	L3	correct	45	L1	L2	L3	correct
15	L1	L2	L3	correct	46	L3	L1	L2	correct
16	L1	L2	L3	correct	47	L1	L2	L3	correct
17	L1	L2	L3	correct	48	L1	L2	L3	correct
18	L1	L2	L3	correct	49	L1	L2	L3	correct
19	L2	L3	L1	correct	50	L1	L2	L3	correct
20	L2	L1	L3	correct	51	L1	L2	L3	correct
21	L2	L3	L1	correct	52	L2	L3	L1	correct
22	L1	L2	L3	correct	53	L1	L2	L3	correct
23	L2	L1	L3	correct	54	L1	L2	L3	correct
24	L2	L3	L1	correct	55	L1	L2	L3	correct
25	L1	L2	L3	correct	56	L1	L2	L3	correct
26	L2	L3	L1	correct	57	L1	L2	L3	correct
27	L1	L2	L3	correct	58	L1	L2	L3	correct
28	L3	L1	L2	correct	59	L1	L2	L3	correct
29	L1	L2	L3	correct	60	NaN	NaN	NaN	unidentified
30	L2	L1	L3	correct	61	NaN	NaN	NaN	unidentified
31	L1	L2	L3	correct	62	NaN	NaN	NaN	unidentified

5. Discussion and Conclusions

The mathematical modeling of a distribution system requires both detailed technical parameterization of individual network elements and the quantification of the power flows over the time. Especially in the case of a complex dense-mesh topology, detailed mapping of LV customer behavior is needed for the purpose of the model verification and its credibility. Even though the following conclusions are mainly the beneficial inputs for this specific model, from the global point of view, it also contributes to finding the interdependencies of power flows over time in more detail.

From the analysis of all transformers the results show:

- the higher power load is achieved on the Weekdays than on the Weekend, specifically 75% of all single-phase active powers range up to 40 kW on the Weekdays and 28 kW on the Weekend;
- the ratio of the supplied and the consumed reactive power is 40/60 on the Weekdays and 50/50 on the Weekend;
- the transformers with a higher power load do not show the changes of the reactive power character. Specifically, there is only the consumed reactive power and no supplied one; and,
- in general, for the transformers with a low power load the supplied reactive power is inversely proportional to the consumed active power.

In the case of the analyses of limit states based on detailed results for the transformer with the maximal power load (T47) and the minimal power load (T61), the following can be observed.

For T47 with maximal power load and with no change of the reactive power character the results show:

- it operates 35% of time with tan *phi* < 1 (on the Weekdays). It also operates 100% of time with tan *phi* > 1 at the level of phase L2 and L3, and it operates at L1 with tan *phi* > 1 approx. for 95% of time (on the Weekend);
- the active and reactive power during the Weekdays is approximately 20% and 4% higher than during the Weekend;
- the active and reactive powers in the individual phases are relatively even;
- in more detail, these summary weekdays and weekend power flows are comparable to those that were achieved during time interval C (08:00:00–15:59:59) and D (16:00:00–21:59:59) with differences of approximately 1–3% for the Weekdays and approximately 1–4% for the Weekend at the same parts of the week; and,
- the summary power flows are higher than during interval A (22:00:00–03:59:59) and B (4:00:00–07:59:59). Specifically, for the active and reactive power up to 29% and 8% during the Weekdays and 10% and 5% during the Weekend.

For T61 with minimal power load and with the change of the reactive power character the results shown:

- it always operates with tan *phi* < 1 at the level of individual phases, when the minimum active power is not less than the maximum reactive power value in a given interval;
- over the Weekend it has an approx. twofold increase in frequencies of the supplied reactive power in individual phases than during the Weekdays; and,
- the active power during the Weekdays is usually 11–33% higher than during the Weekend and for the reactive power the differences are in range 1–54%, but in terms of the absolute values these are comparable to differences for the transformer T47.

Furthermore, a novel approach that is presented in this article is the demonstration of the phase unification within the measurements of the short-term voltage drops that were recorded by PQ monitors instead of the most often used process demanding HW or SW techniques. Unlike these techniques, the shown approach is not both computationally demanding, because no complex evaluation of the continuous voltage trends are observed and also financially demanding because it used installed PQ monitors and no additional HW is required to be installed within the distribution system. Although the results show the ability to identify phases in 100% of the cases, this approach has still to be verified via DSO in the real distribution system and, as a result of the application of the short-term voltage drops, there is also a risk that no voltage events will generally occur. The analysis of statistically sufficient sample of data (at least 1 year) is also necessary in order to relevantly assess the DS behaviour based on long-term measured values from DTS.

Moreover, the results show that it is not necessary to assess the voltage magnitudes while using the measuring over the unified phase data. On the other hand, the unified data can provide better information in which particular phase the voltage tolerance is compliant/non-compliant, thus the complex dependences can be generally observed in the context of a whole distribution system.

The results also have a practical contribution directly to the DSO. The main operating criterion of the analyzed municipal distribution system has not been complexly evaluated prior to the installation of PQ monitors. Thus, the results confirm the fulfilment of the established criterion and the power load of all transformers is below the required upper limit of 50% of S_n. It should be noted that the power load has always to be calculated from the rms/trms voltage and current values. Unlike other incorrect approaches, this takes the influence of the process of data aggregation and the change of the reactive power character in the measurement interval into account as well.

References

1. Dileep, G. A survey on smart grid technologies and applications. *Renew. Energy* **2020**, *146*, 2589–2625. [CrossRef]

2. Pau, M.; Patti, E.; Barbierato, L.; Estebsari, A.; Pons, E.; Ponci, F.; Monti, A. A cloud-based smart metering infrastructure for distribution grid services and automation. *Sustain. Energy Grids Netw.* **2018**, *15*, 14–25. [CrossRef]

3. Zhichao, L.; Yuping, Z. Research on Distribution Network Operation and Control Technology Based on Big Data Analysis. In Proceedings of the 2018 China International Conference on Electricity Distribution (CICED), Tianjin, China, 17–19 September 2018; pp. 1158–1161.

4. Guo, Y.; Lin, T.; Liang, K.; Chen, G. Network Quality Monitoring for Typical Power Services. In Proceedings of the 2019 IEEE 3rd Information Technology, Networking, Electronic and Automation Control Conference (ITNEC), Chengdu, China, 15–17 March 2019; pp. 1437–1441.

5. Zhao, Z.; Zheng, R.R.; Xing, N.Z. The research on 35kV power station service data flow model in power grid network. In Proceedings of the 2014 International Conference on Information Science, Electronics and Electrical Engineering, Sapporo, Hokkaido, Japan, 26–28 April 2014; pp. 24–27.

6. Rudin, C.; Waltz, D.; Anderson, R.N.; Boulanger, A.; Salleb-Aouissi, A.; Chow, M.; Dutta, H.; Gross, P.N.; Huang, B.; Ierome, S.; et al. Machine Learning for the New York City Power Grid. *IEEE Trans. Pattern Anal. Mach. Intell.* **2012**, *34*, 328–345. [CrossRef] [PubMed]

7. Martinez-Pabon, M.; Eveleigh, T.; Tanju, B. Smart Meter Data Analytics for Optimal Customer Selection in Demand Response Programs. *Energy Procedia* **2017**, *107*, 49–59. [CrossRef]

8. Wan Yen, S.; Morris, S.; Ezra, M.A.G.; Jun Huat, T. Effect of smart meter data collection frequency in an early detection of shorter-duration voltage anomalies in smart grids. *Int. J. Electr. Power Energy Syst.* **2019**, *109*, 1–8. [CrossRef]

9. Liao, Y.; Weng, Y.; Liu, G.; Rajagopal, R. Urban MV and LV Distribution Grid Topology Estimation via Group Lasso. *IEEE Trans. Power Syst.* **2019**, *34*, 12–27. [CrossRef]

10. Elphick, S.; Ciufo, P.; Drury, G.; Smith, V.; Perera, S.; Gosbell, V. Large Scale Proactive Power-Quality Monitoring: An Example from Australia. *IEEE Trans. Power Deliv.* **2017**, *32*, 881–889. [CrossRef]

11. Mertens, E.A.; Dias, L.F.S.; Fernandes, F.A.; Bonatto, B.D.; Abreu, J.P.G.; Arango, H. Evaluation and trends of power quality indices in distribution system. In Proceedings of the 2007 9th International Conference on Electrical Power Quality and Utilisation, Barcelona, Spain, 9–11 October 2007; pp. 1–6.

12. Xuemei, Y.; Jinliang, J. Study on power supply of ring network of 10KV distribution network. In Proceedings of the 2008 China International Conference on Electricity Distribution, Guangzhou, China, 10–13 December 2008; pp. 1–5.

13. Tao, X.; Renmu, H.; Peng, W.; Dongjie, X. Applications of data mining technique for power system transient stability prediction. In Proceedings of the 2004 IEEE International Conference on Electric Utility Deregulation, Restructuring and Power Technologies. Proceedings, Hong Kong, China, 5–8 April 2004; pp. 389–392.

14. Schäfer, F.; Menke, J.; Braun, M. Contingency Analysis of Power Systems with Artificial Neural Networks. In Proceedings of the 2018 IEEE International Conference on Communications, Control, and Computing Technologies for Smart Grids (SmartGridComm), Aalborg, Denmark, 29–31 October 2018; pp. 1–6.

15. Tinney, W.F.; Hart, C.E. Power Flow Solution by Newton's Method. *IEEE Trans. Power Appar. Syst.* **1967**, *PAS-86*, 1449–1460. [CrossRef]

16. Stott, B.; Alsac, O. Fast Decoupled Load Flow. *IEEE Trans. Power Appar. Syst.* **1974**, *PAS-93*, 859–869. [CrossRef]

17. Stott, B. Decoupled Newton Load Flow. *IEEE Trans. Power Appar. Syst.* **1972**, *PAS-91*, 1955–1959. [CrossRef]

18. Rao, S.; Feng, Y.; Tylavsky, D.J.; Subramanian, M.K. The Holomorphic Embedding Method Applied to the Power-Flow Problem. *IEEE Trans. Power Syst.* **2016**, *31*, 3816–3828. [CrossRef]

19. Bokhari, A.; Alkan, A.; Dogan, R.; Diaz-Aguiló, M.; De Leon, F.; Czarkowski, D.; Zabar, Z.; Birenbaum, L.; Noel, A.; Uosef, RE. Experimental Determination of the ZIP Coefficients for Modern Residential, Commercial, and Industrial Loads. *IEEE Trans. Power Deliv.* **2014**, *29*, 1372–1381. [CrossRef]

20. Hala, T.; Drapela, J. On stabilization of voltage in LV distribution system employing MV/LV OLTC transformer with control based on Smart Metering. In Proceedings of the 2019 20th International Scientific Conference on Electric Power Engineering (EPE), Ostrava, CR, VŠB-Technical University of Ostrava, Ostrava, Czech Republic, 15–17 May 2019; pp. 1–6.

21. Vycital, V.; Ptacek, M.; Toman, P.; Topolanek, D.; Drapela, J.; Zamphiropolos, J. Phase identification in smart metering pilot project Komorany. In *CIRED 2019, CIRED—Open Access Proceedings Journal, Proceedings of the 25th International Conference and Exhibition on Electricity Distribution, Madrid, Spain, 3–6 June 2019*; AIM: El Segundo, CA, USA, 2019.

22. Chen, C.S.; Ku, T.T.; Lin, C.H. Design of phase identification system to support three-phase loading balance of distribution feeders. In Proceedings of the 2011 IEEE Industrial and Commercial Power Systems Technical Conference, Baltimore, MD, USA, 1–5 May 2011; pp. 1–8.

23. Shen, Z.; Jaksic, M.; Mattavelli, P.; Boroyevich, D.; Verhulst, J.; Belkhayat, M. Three-phase AC system impedance measurement unit (IMU) using chirp signal injection. In Proceedings of the 2013 Twenty-Eighth Annual IEEE Applied Power Electronics Conference and Exposition (APEC), Long Beach, CA, USA, 17–21 March 2013; pp. 2666–2673.

24. Pappu, S.J.; Bhatt, N.; Pasumarthy, R.; Rajeswaran, A. Identifying topology of low voltage distribution networks based on smart meter data. *IEEE Trans. Smart Grid* **2018**, *9*, 5113–5122. [CrossRef]

25. Dilek, M.; Broadwater, R.P.; Sequin, R. Phase prediction in distribution systems. In Proceedings of the 2002 IEEE Power Engineering Society Winter Meeting, New York, NY, USA, 27–31 January 2002; pp. 985–990.

26. Arya, V.; Seetharam, D.; Kalyanaraman, S.; Dontas, K.; Pavlovski, C.; Hoy, S.; Kalagnanam, J.R. Phase identification in smart grids. In Proceedings of the 2011 IEEE International Conference on Smart Grid Communications (SmartGridComm), Brussels, Belgium, 17–20 October 2011; pp. 25–30.

27. Pezeshki, H.; Wolfs, P. Correlation based method for phase identification in a three phase LV distribution network. In Proceedings of the 2012 22nd Australasian Universities Power Engineering Conference (AUPEC), Bali, Indonesia, 26–29 September 2012; pp. 1–7.

28. Short, T.A. Advanced metering for phase identification, transformer identification, and secondary modeling. *IEEE Trans. Smart Grid* **2013**, *4*, 651–658. [CrossRef]

29. Wen, M.H.; Arghandeh, R.; von Meier, A.; Poolla, K.; Li, VO. Phase identification in distribution networks with micro-synchrophasors. In Proceedings of the 2015 IEEE Power & Energy Society General Meeting, Denver, CO, USA, 26–30 July 2015; pp. 1–5.

30. Seal, B.K.; McGranaghan, M.F. Automatic identification of service phase for electric utility customers. In Proceedings of the 2011 IEEE Power and Energy Society General Meeting, Detroit, MI, USA, 24–28 July 2011; pp. 1–3.

31. Lv, J.; Pawlak, M.; Annakkage, U.D.; Bagen, B. Statistical testing for load models using measured data. *Electr. Power Syst. Res.* **2018**, *163*, 66–72. [CrossRef]

32. Srinivasan, K.; Lafond, C. Statistical analysis of load behavior parameters at four major loads. *IEEE Trans. Power Syst.* **1995**, *10*, 387–392. [CrossRef]

33. Loewenstern, Y.; Katzir, L.; Shmilovitz, D. Statistical analysis of power systems and application to load forecasting. In Proceedings of the 2014 IEEE 28th Convention of Electrical & Electronics Engineers in Israel (IEEEI), Eilat, Israel, 3–5 December 2014; pp. 1–5.

34. Ahmed, M.A.; Reddy, K.S.; Prakash, J.; Rai, A.; Singh, B.P. Statistical analysis of load and its frequency response for load forecasting in a medium voltage distribution system. In Proceedings of the 2017 International Conference on Energy, Communication, Data Analytics and Soft Computing (ICECDS), Chennai, India, 1–2 August 2017; pp. 1146–1149.

35. Seppala, A. Statistical distribution of customer load profiles. In Proceedings of the 1995 International Conference on Energy Management and Power Delivery EMPD '95, Singapore, 21–23 November 1995; pp. 696–701.

36. Dong, Z.; Wang, Y.; Zhao, J. Variational Bayesian inference for the probabilistic model of power load. *IET Gener. Transm. Distrib.* **2014**, *8*, 1860–1868. [CrossRef]

37. Singh, R.; Pal, B.C.; Jabr, R.A. Statistical Representation of Distribution System Loads Using Gaussian Mixture Model. *IEEE Trans. Power Syst.* **2010**, *25*, 29–37. [CrossRef]

38. Ganjavi, A.; Christopher, E.; Johnson, C.M.; Clare, J. A study on probability of distribution loads based on expectation maximization algorithm. In Proceedings of the 2017 IEEE Power & Energy Society Innovative Smart Grid Technologies Conference (ISGT), Washington, DC, USA, 23–26 April 2017; pp. 1–5.

39. Ahmad, A.; Azmira, I.; Ahmad, S.; Anwar Apandi, N.I. Statistical distributions of load profiling data. In Proceedings of the 2012 IEEE International Power Engineering and Optimization Conference, Melaka, Malaysia, 6–7 June 2012; pp. 199–203.

40. European standard EN 50160 ed.3, Voltage Characteristics of Electricity Supplied by Public Distribution Systems. 2003. Available online: https://www.orgalim.eu/position-papers/en-50160-voltage-characteristics-electricity-supplied-public-distribution-system (accessed on 14 March 2003).

41. International Electrotechnical Commission. Electromagnetic compatibility (EMC)-Part 4-30: Testing and measurement techniques-Power quality measurement methods. Available online: https://ci.nii.ac.jp/naid/10026582038/ (accessed on 10 October 2019).

42. *IEC 62053-23, Electricity Metering Equipment (a.c.)—Particular Requirements—Part 23: Staticmeters for Reactive Energy (Classes 2 and 3)*; International Electrotechnical Commission: Geneva, Switzerland, 2018.

43. *IEC 62056-6-1, Electricity Metering Data Exchange—The DLMS/COSEM Suite—Part 6-1: Object Identification System (OBIS)*; International Electrotechnical Commission: Geneva, Switzerland, 2017.